Energetic charged particle yields induced by pions on complex nuclei*

H. E. Jackson, S. B. Kaufman, L. Meyer-Schützmeister, J. P. Schiffer,† S. L. Tabor, S. E. Vigdor,‡ and J. N. Worthington
Argonne National Laboratory, Argonne, Illinois 60439

L. L. Rutledge, Jr. and R. E. Segel§
Northwestern University,¶ Evanston, Illinois 60201

R. L. Burman, P. A. M. Gram, R. P. Redwine, and M. A. Yates
Los Alamos Scientific Laboratory, Los Alamos, New Mexico 87545

(Received 7 February 1977)

The spectra of protons ($60 < E_p < 200$ MeV) and deuterons (80 MeV $< E_d$) produced by 100- and 220-MeV π^+ and π^- on Al, Ni, and Ta targets were measured. The shapes of proton spectra are similar for π^+ and π^-, with absolute yields in $\sim 3:1$ ratio; the yields vary as $\sim A^{2/3}$. The exception is the forward-angle yield at 100 MeV where the proton spectra with π^+ are different in shape from π^-, the yield ~ 5 times as high, and the target dependence is $\sim A^{1/3}$. This pattern is not readily understood at the present time.

[NUCLEAR REACTIONS ^{27}Al, ^{62}Ni, ^{181}Ta, $(\pi^{\pm},p)$, and $(\pi^{\pm},d)$. $E_\pi = 100$, 220 MeV, $\theta = 45$, 94°; measured $d^2\sigma/d\Omega dE$ for $50 < E_p < 200$ MeV and $80 < E_d < 200$ MeV.]

I. INTRODUCTION

Our knowledge of the mechanisms whereby energetic pions interact with complex nuclei is very limited. We have some experimental information on elastic scattering[1] and some on total reaction cross sections.[2] However, there are almost no data which indicate how the reaction cross section is divided between inelastic scattering and charge exchange on one hand, and true absorption, where the pion gives up its rest mass, on the other. Some data on the spectrum of gamma rays seen from pion interactions with complex nuclei indicate that indeed a large part of the reaction cross section is likely to be absorption.[3] The only model with detailed predictions concerning pion-nucleus reactions is the intranuclear cascade calculation[4] which has recently been modified.[5]

The spectrum of energetic protons emerging from a nucleus is a good measure of the absorption process. The momentum of a 100–200-MeV pion is small (corresponding to a 20–50-MeV nucleon) and single-scattering collisions could not produce many nucleons with energies higher than 50 MeV. Some work has been done studying coincident collinear nucleons from pions interacting with light nuclei,[6] and from stopped π^- beams.[7] With 135-MeV π^+ on ^{12}C, Belotti, Cowall, and Mateazzi[8] find that in a large fraction (~55%) of the pion absorption events more than two charged particles are emitted, and fewer than 35% of the absorption events give two energetic ($E_p > 50$ MeV) charged particles. One recent experiment has been carried out measuring protons from 235-MeV π^+ on Ni without further coincidence requirements.[9] The results were in rather drastic disagreement with cascade calculations in that the yield of protons seemed to drop much faster with increasing energy than the calculation predicted.[4] The more recent cascade calculations[5] seemed to describe these data somewhat better, though for 100-MeV protons (the highest energy detected in Ref. 9) there still seems to be a discrepancy of about a factor of 2.

A proton spectrum in which the number of protons falls off more rapidly with energy than the cascade calculations predict might suggest that absorption does not proceed through the two step $(\pi + N \rightarrow N^*,\ N^* + N \rightarrow N + N)$ process implicit in the calculations. It was a desire to better understand the absorption process and the overall pion-nucleus reaction mechanisms that motivated the present measurement. We attempted to measure the spectrum of protons to energies well above the 100-MeV cutoff of Amann *et al.*[9] and to get some information on the dependence of the proton yield on target mass, pion energy, angle, and pion charge.

II. EXPERIMENTAL METHOD

The pion beam of the low-energy pion channel at the Los Alamos Meson Physics Facility was used.[10] The properties of this beam, the location of the focus, the beam size, and the contaminants are well known. At both 100- and 220-MeV pion energy a beam of known purity and a spot size of

~2×3 cm (containing >95% of the beam) is obtained. The momentum slits were adjusted for beam intensities of ~5×10^5 pions/sec. Spectra were collected with ~2×10^9 incident pions.

A. Detector system

The proton detector was a conventional ΔE-E counter telescope illustrated in Fig. 1. Scintillator B defined the solid angle for particles entering the detector from the vicinity of the target and scintillator A was the ΔE counter. The E counter was a 12.7-cm-diam×10.2-cm-deep NaI crystal. Protons with kinetic energy up to 190 MeV were stopped in the telescope. We report proton spectra over the range 60–190 MeV, the lower limit being set by the point at which the correction for energy loss by protons in the target becomes large. The detector solid angle was ~30 msr.

The occurrence of a triple coincidence A·B·(NaI) caused the analog pulses from counter A and the NaI to be gated into a pair of analog-to-digital converters. Digitized pulse-height information was stored in a 32×256 element array in a PDP 11/45 computer.

The NaI counter was equipped with a light-emitting diode (LED) light pulser. The light converter was placed on the edge of the transparent plate that adapts the flat surface of the NaI crystal container to the curved surface of the phototube. From this vantage point, the light from the converter illuminated the entire photocathode. This controlled light source was used in two ways: (1) to measure variation in gain, and (2) to estimate detector inefficiencies caused by pileup and other rate-dependent effects.

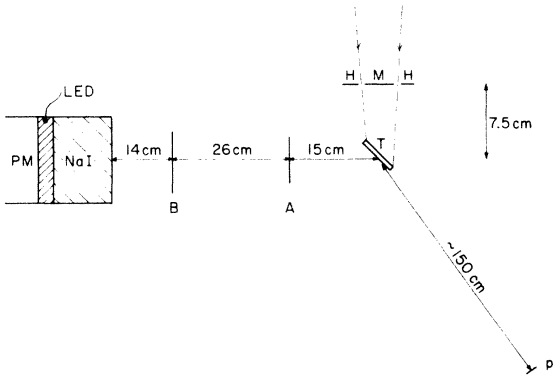

FIG. 1. Schematic diagram of the experimental layout. The outer edges of the beam are shown by dashed lines, T indicates the target. Counter M is the beam monitor scintillator, H are halo counters used to monitor the beam position. B and A are the solid-angle defining and the ΔE scintillators, respectively, and scintillator p supplies pulses during the beam burst for the LED.

B. Targets

The targets consisted of metal plates (~2.1×3.5 cm×1.8 g/cm² of >99% enriched ^{62}Ni, 2.1×4.0 cm ×0.88 g/cm² of ^{27}Al, and 2.1×3.9 cm×1.33 g/cm² of ^{181}Ta) placed at 45° with respect to the incident beam. The thickest of these, the ^{62}Ni target, corresponds (at 45°) to the range of ~42-MeV protons and ~56-MeV deuterons. Corrections had to be made to the energy spectra obtained from the NaI detector to compensate for the energy loss in the target and in the scintillators A and B.

C. Beam monitoring

Two methods of beam monitoring were used. One was to integrate the anode current of a photomultiplier that viewed a plastic scintillator placed 3.7 cm upstream from the target, and which was slightly larger than the target in order to compensate for the convergence of the beam. A correction factor (≲15%) was applied to the integrator counts in those cases where the beam and target geometry indicated that the target would intercept an appreciably different fraction of the beam. This scintillator was also viewed by a photomultiplier tube that could be operated at a higher voltage and count individual pulses. The integrated current was calibrated at low beam against the scaled counts in the scintillator. This system was found to be stable to better than 5%.[11] The second method was to place a piece of Pilot B plastic, the same size as the target, in the target position, and counting the amount of ^{11}C activity produced by a β^+-annihilation radiation coincidence measurement. The ^{11}C production cross sections of Ref. 12 were used to calculate the flux. The absolute number of incident pions as determined by these two methods agreed to within 5%.

D. Energy calibration

In order to establish the energy scale in the NaI detector several measurements were conducted. The LEP channel was run without an absorber, thus providing protons of 56.8 MeV. These protons were scattered at 45° into the detector by a 0.2-g/cm² Fe target. Higher energy calibration points were obtained at $E_p\approx150$ MeV, from the $\pi^+ + D \rightarrow 2p$ reaction; a CD_2 target was used and an 18-cm×18-cm scintillation counter was placed at the appropriate angle with the NaI telescope in order to detect the coincident outgoing protons. A complication arose in the energy calibration because of the magnetic fringe fields around the LEP channel, which resulted in small gain shifts (≲15%) in the NaI phototube when the channel settings were

changed. The necessary corrections to the energy scale were made by monitoring the LED pulser peak. The degree of consistency of the four energy calibrations implies an uncertainty in the energy scale of at most ±5%.

E. Dead-time monitoring

In order to monitor dead-time effects the light-emitting diode mounted on the light pipe connecting the NaI crystal to the phototube was operated by pulses that were triggered by scattered particles detected in a scintillator placed ~150 cm from the target at about 45°. Thus the calibration pulses were provided during the actual beam pulse. With each triggering event an electronic pulse was also provided to the ΔE preamplifier. The number of such pulses was recorded on a scaler as well as summed in the spectrum. The correction for dead time was generally between 5 and 20%.

F. Data collection

The E-ΔE spectra were stored in a 32×256-channel array in a PDP 11/45 computer. The LED pulses were stored in a region of this array where they were expected to interfere least with the real events. A typical spectrum is shown in Fig. 2. The protons are clearly resolved from deuterons and pions. Some evidence for heavier particles is seen, though the experiment was not designed for these, and the targets were generally too thick for the heavier particle spectra to be meaningful. A slice of the two-parameter spectrum showing the separation in ΔE for a narrow slice in E is shown in Fig. 3. The pions were generally not stopped in the NaI. It is possible that some pulses appearing as high-energy protons might be caused by pions that had sufficiently low energy to give a ΔE signal similar to that of a proton, but which then underwent a nuclear reaction in the NaI, giving a big pulse in that detector. This possibility was checked by lowering the beam intensity and allowing the pion beam to enter the NaI telescope directly. The resultant spectrum of spurious protonlike events is shown in Fig. 4 together with the full proton spectrum obtained in a normal run, the two spectra are normalized so that the total number of pionlike pulses was the same. Clearly this source of background is negligible.

It should be noted further that, unlike the experiment of Amann *et al.*,[9] no anticoincidence counter was used to exclude the protons with energies too high ($E_p \gtrsim 200$ MeV) to be stopped in the NaI detector. Including such events has the advantage that all protons above ~50 MeV will have been detected, although the spectrum may become somewhat distorted since a proton with energy greater than 200 MeV will deposit less than its full energy in the scintillator. However, since the number of such protons is expected to be small, such distortions should not be very serious.

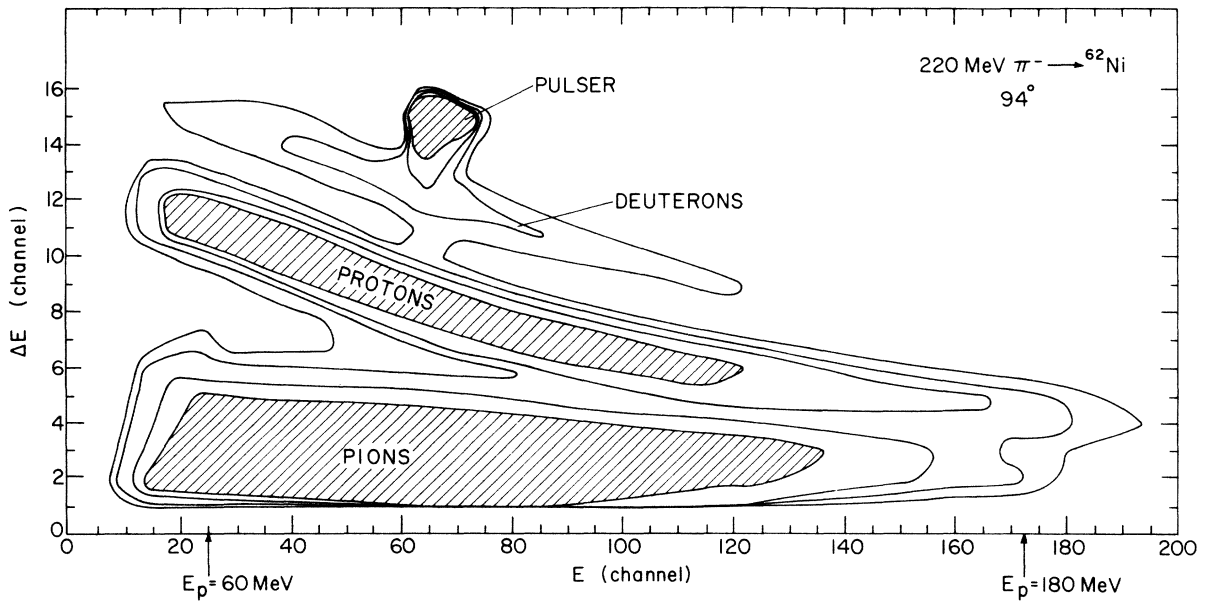

FIG. 2. Contour plot of a typical spectrum. Contours are drawn for every factor of 2 starting with 25 counts; the shaded areas are the regions with over 200 counts/bin. The pulser peak is from the LED device. Two proton energies are indicated.

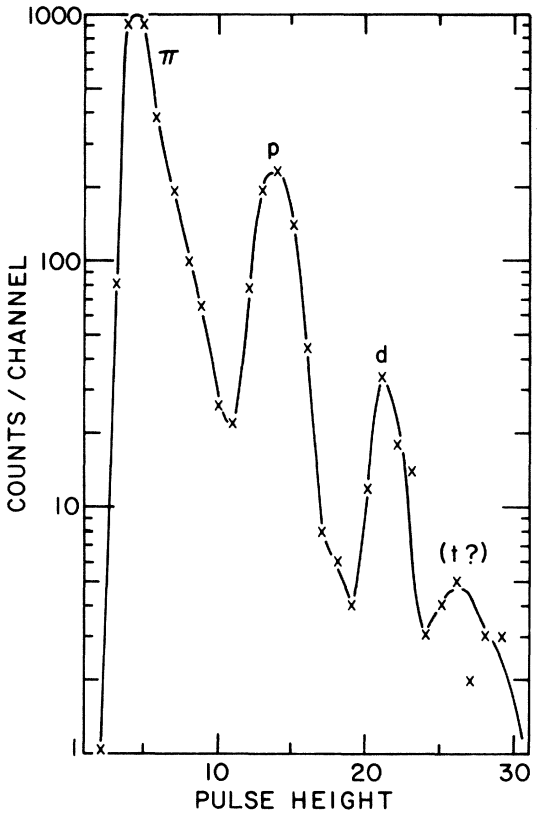

FIG. 3. A spectrum from the ΔE detector with a fixed energy deposited in the NaI. The pion, proton, and deuteron peaks are so labeled, the weak (t?) peak may be tritons. The ΔE channels are expanded by a factor of 2 compared to Fig. 2.

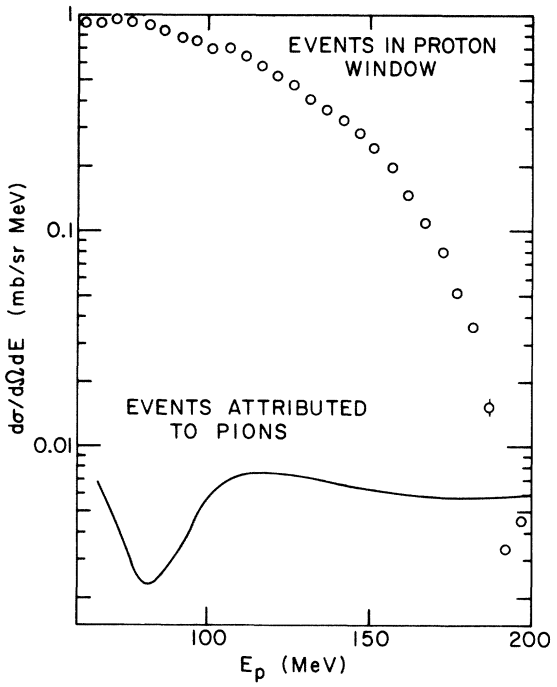

FIG. 4. Spectrum of pulses corresponding to the "proton window" in the E-ΔE plane. The line represents contributions from pions that produce a reaction in the NaI and give rise to background events within the proton window; it was obtained by allowing a small pion beam at $E_\pi = 30$, 60, 100, and 220 MeV to impinge directly into the telescope. The minimum in this pion contribution is a consequence of the shape of the proton window and the behavior of low-energy pions. The relative scales are accurate to ~a factor of 2.

G. Corrections to the particle spectra

The spectra had to be corrected for energy loss in the target and in the plastic ΔE and defining scintillators, and also for the gain shifts caused by the magnetic fringe fields. In addition, corrections were made for reactions in the NaI according to the measurements and calculations of Goulding and Rogers.[13] These corrections amount to at most 30% at the highest proton energies. Corrections were also made for events due to pions in the detector as indicated in Fig. 4. The resultant uncertainties are estimated to be about ±20% in cross section and ±5% in the energy scales obtained.

H. Description of the data

Spectra were obtained for the ^{27}Al, ^{62}Ni, and ^{181}Ta targets at 45° and 94° for π^+ and π^- beams at 100 and 220 MeV. In addition, one spectrum was measured at 120° on ^{62}Ni and one at 90° on ^{12}C, both with 220-MeV π^+. A typical proton spectrum is shown in Fig. 5 with the error bars on the yields and the energy scale indicated. These include both statistical errors and estimates of systematic errors. This spectrum disagrees with that published by Amann *et al.*[9] for similar conditions (235- instead of 220-MeV pions, natural Ni instead of ^{62}Ni, 90° instead of 94°). However, the group who performed the experiment in Ref. 9 recently repeated this measurement and obtained a proton spectrum whose shape is more consistent with that shown in Fig. 5.[14]

The trends in the data are displayed in various ways in Figs. 6–8, and the cross sections for protons above 60 MeV are given in Table I. It should be noted that all cross sections, energies, and angles are quoted in the laboratory system, since with possible multibody reactions this avoids ambiguities. In any case, the coordinate transformations would modify these results only minimally ($\lesssim$5% for Al in cross section and shifts of $< 1°$ in $\theta_{\text{c.m.}}$ compared with θ_{lab}). Several features may be noted:

(i) The shapes of the proton spectra for a given energy, charge, and angle are largely independent

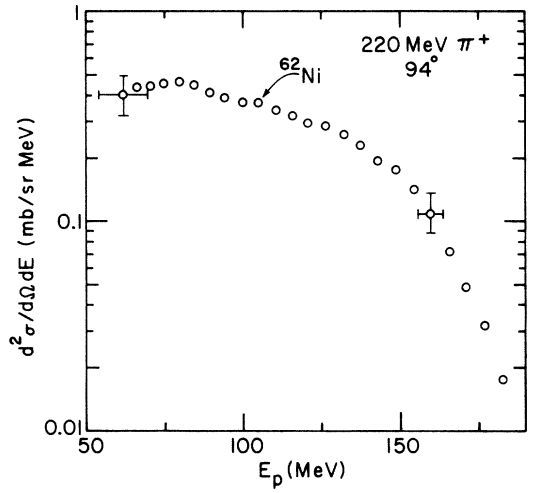

FIG. 5. A typical spectrum of protons obtained for ^{62}Ni. Error bars in cross section and energy are shown near the top and bottom of the spectrum.

of target mass. The cross sections scale approximately as $A^{2/3}$, except for the 100-MeV π^+ data at 45° which vary more nearly as $A^{1/3}$. This point is illustrated in Fig. 6.

(ii) The shapes of the proton spectra for a given energy and angle seem to be approximately independent of the incident pion charge as may be seen in Fig. 7. The magnitude seems to be a factor of ~3 larger for π^+ than π^-. The exception again is at

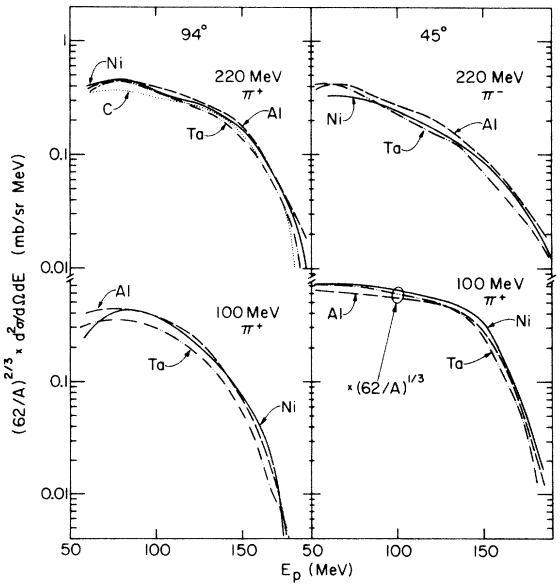

FIG. 6. Shapes of spectra for various targets. To show the similarity all the cross sections were multiplied by $(62/A)^{2/3}$, except for the 100-MeV 45° data, where $(62/A)^{1/3}$ was used.

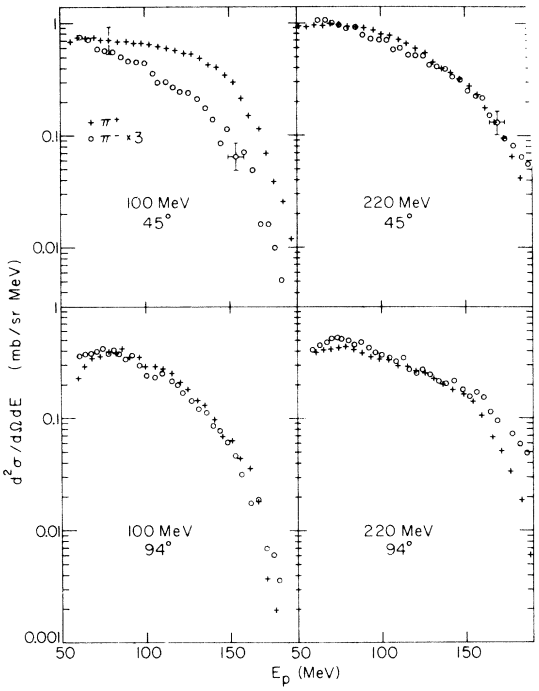

FIG. 7. Comparison of π^+ and π^- data for ^{62}Ni. To emphasize the similarity the π^- cross sections were multiplied by a factor of 3. Typical error bars are shown.

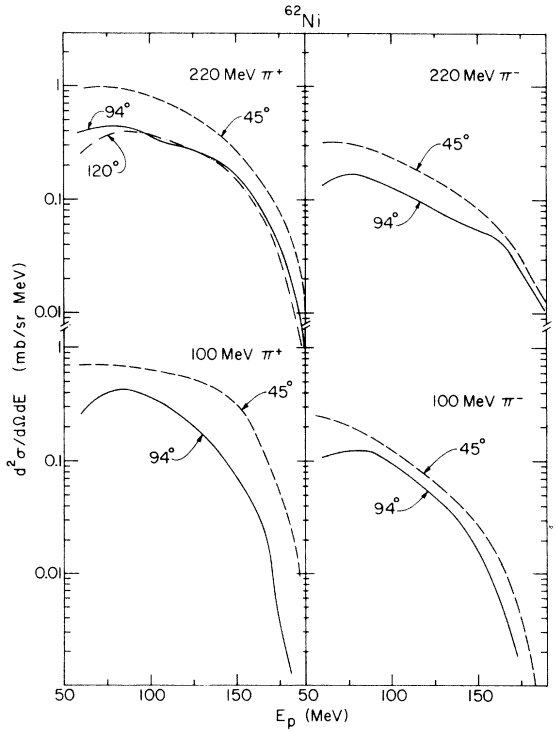

FIG. 8. The angle dependence of proton yield for the ^{62}Ni target.

TABLE I. Cross sections in mb/sr (the errors are about ±20%) for producing protons with $E_p \geq 60$ MeV.

E_π, θ (MeV)	^{12}C	^{27}Al		^{62}Ni		^{181}Ta	
	π^+	π^+	π^-	π^+	π^-	π^+	π^-
100, 45°		39	6.5	57	11.0	78	17.8
100, 94°		16.3	4.0	26	7.0	48	13.8
220, 45°		48	14.5	70	26	130	46
220, 94°	9.7	19.6	6.7	33	12.2	66	24
220, 120°				35			

100 MeV, especially at 45°. This may also be seen in Table II.

(iii) The angular distributions of protons over the whole proton energy range seem mildly forward peaked (Fig. 8).

Deuteron spectra were also obtained, though the incomplete separation from the protons introduces a slightly larger uncertainty here. Because of the thickness of targets and detectors the deuteron spectra are meaningful only above 80 MeV. The shapes of the spectra are again independent of the target and *both* the magnitudes and shapes of the spectra seem to be approximately independent of pion charge. The angle and energy dependence of the deuteron spectra are shown in Fig. 9, the relative cross sections as a function of target mass are shown in Table III.

III. DISCUSSION

A. Some simple considerations

It is not clear what relative yields to expect of protons from π^+ and π^- absorption in nuclear matter. If absorption occurs on a pair of nucleons, with a probability independent of the spin or isospin of the pair, and if one neglects nucleon-nucleon correlations, then one would expect 5 times as many protons from π^+ as from π^-. [n-p pairs are twice as abundant as n-n (or p-p) pairs, and a π^+ yields two protons when it absorbs on an n-p pair and only one from an n-n pair, while a π^- only yields a proton when it absorbs on a p-p pair.]

TABLE II. Ratio of cross sections for producing protons: $\sigma_{\pi^+}/\sigma_{\pi^-}$. The uncertainties in these ratios are about ±20%.

E_π, θ (MeV)	^{12}C [a]	^{27}Al	^{62}Ni	^{181}Ta
100, 45°		6.0	5.2	4.4
100, 94°		4.1	3.8	3.5
130	~3.6			
220, 45°		3.3	2.7	2.8
220, 94°		2.9	2.7	2.7

[a] From Ref. 8.

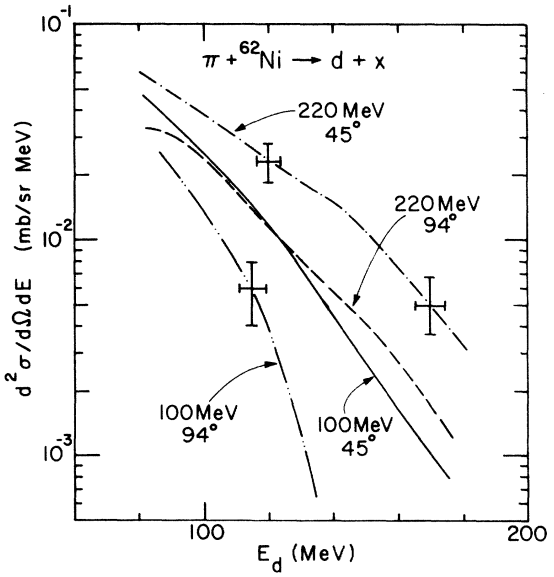

FIG. 9. Deuteron spectra from the ^{62}Ni target with typical error bars shown. The spectra are indistinguishable between π^+ and π^-, the difference in integral yields in Table III is barely significant.

If the absorption depends on the spin-isospin of the nucleon pair, and if correlations are introduced, this ratio becomes modified. The ratio would be 3 if absorption could only take place with a pair of nucleons in an initial $T = 1$ state and no change in isospin; it would be infinite for the $T = 0$ state. There is no reason to expect the $T = 1$ state to dominate.

If, on the other hand, one assumes that absorption proceeds by the pion first forming a $\Delta(\frac{3}{4}, \frac{3}{2})$ resonance, and then by a subsequent Δ-nucleon collision yielding two nucleons, one would expect a ratio of 11 : 1 for $N \approx Z$. (The cross section for $\pi^+ + p \rightarrow \Delta^{++}$ is 3 times that for $\pi^+ + n \rightarrow \Delta^+$, while the ratio for the three processes $\Delta^{++} + n \rightarrow 2p : \Delta^+ + p \rightarrow 2p : \Delta^+ + n \rightarrow p + n$ is 3 : 1 : 2 from simple isospin considerations. The 11 : 1 ratio follows upon noting that the number of protons from π^- absorption is, by charge symmetry, equal to the number of neutrons from π^+ absorption.)

The interpretation of the observed 3 : 1 ratio of π^+/π^- yields depends critically on whether the spectrum of emerging nucleons is characteristic of the primary absorption event or whether it is modified by considerable scattering and cascading (including nucleon charge exchange). Several facts support the argument that the observed nucleon spectrum is likely to be dominated by the primary nucleons from the pion absorption.

(a) It is fairly well accepted[15] that the mean free path of a nucleon of ~100 MeV in a nucleus is ~5 fm for undergoing any inelastic collision.[16] The

TABLE III. Cross sections in mb/sr (uncertainties in these cross sections are about ±25%) for producing deuterons with $E_d \geq 80$ MeV.

E_π, θ (MeV)	^{12}C	^{27}Al		^{62}Ni		^{181}Ta	
	π^+	π^+	π^-	π^+	π^-	π^+	π^-
100, 95° [a]		1.0(25)	0.9	1.5(26)	1.4	2.9(37)	2.1
100, 94°		0.40(24)	0.38	0.9(33)	0.56	1.5(33)	1.2
220, 45°		1.5(31)	1.6	2.9(41)	2.7	4.6(35)	4.9
220, 94° [a]	0.34(35)	0.65(36)	0.60	1.3(39)	1.1	2.7(40)	2.2
220, 120°				1.0			

[a] The numbers in parentheses are the ratios of deuterons to protons, multiplied by 1000, in the respective energy ranges covered by the detector.

mean free path for a hard collision, where the nucleon loses an appreciable fraction of its kinetic energy to another nucleon, must be even longer. Thus the observed proton spectrum is likely to be a relatively good representation of the primary nucleon spectrum.

(b) No A-dependence is seen in the π^+/π^- ratios. If the initial ratio were much larger, then the protons actually observed with π^- incident would come from secondary processes and their number, relative to those from π^+, may be expected to vary with the size of the nucleus. No such differences are seen.

(c) With the exception of the 100-MeV 45° data, no significant dependence of the π^+/π^- ratio on outgoing proton energy is observed (Fig. 7). One would expect secondary scattering processes to significantly degrade the energy of the nucleons originating from pion absorption and thus to have an increasing effect on the π^+/π^- ratio with decreasing proton energy. In particular, it seems unlikely than an appreciable fraction of the highest-energy protons (which carry off roughly half the kinetic plus rest mass energy brought in by the pions) could result from secondary scattering; here, the main effect of a cascade would be simply to drain a given fraction of the primary high-energy proton flux, the fraction being independent of the absorbed pion charge, so that the π^+/π^- ratio is still characteristic of the absorption process.

(d) It is also interesting to observe that a heavy nucleus, such as ^{181}Ta, has almost 50% more neutrons than protons, and this difference tends to be accentuated on the surface. One may expect consequent differences in π^+/π^- ratios between heavy and light nuclei, if the nucleon production mechanism is dominated by cascades. Such a trend is not evident in the data shown in Table II. The $\pi^+\pi^-$ ratio was also estimated for 130-MeV pions on ^{12}C from the bubble chamber experiment of Belotti *et al.*[8] They used momentum reconstruction to estimate the neutral spectrum. The ratio of protons to neutrons must be the same as the π^+/π^- ratios for protons. These data include all angles and only energies above 60 MeV were used.

The above arguments do not convincingly rule out a significant role for pion cascades prior to absorption, since the pion mean free path in the nucleus may be considerably shorter than that of a high-energy nucleon, and the energy degradation in such a cascade is likely to represent a small fraction of the *total* (kinetic plus rest-mass) pion energy. Thus pion charge-exchange may contribute to the observed π^+/π^- ratio. Another possible explanation of the 3 : 1 ratio which is consistent with the above observations is that the pion absorption occurs predominantly on a cluster larger than two nucleons. Were the initial process $\pi + \alpha \rightarrow 4N$, for example, the 3 : 1 ratio would follow immediately.

The A dependence of the yield is of further interest because it gives some measure of the extent to which the processes responsible for energetic protons are surface peaked. The cross section for a process where the nucleus is transparent to both incident and outgoing particles should be proportional to A; if the mean-free path becomes short for either the incident or outgoing particle an $A^{2/3}$ dependence may be expected; if absorption is important in both channels then the cross section would change from an $A^{2/3}$ dependence at back angles to $A^{1/3}$ in the forward direction, where only a ring on the periphery of the nucleus could contribute. In Figs. 10 and 11 the A dependence is summarized. It seems that the dependence at 220 MeV is about $A^{2/3}$, while at 100 MeV the rather large forward yield varies approximately as $A^{1/3}$. The observed A dependence is thus consistent with the interpretation of a mean free path which is short for the incident pions but relatively long for the high-energy nucleons.

From Table I one may estimate that at $E_\pi = 220$ MeV on Ni, all neutrons and protons above 60 MeV correspond to a cross section of 750 ± 200 mb. The estimates of the total proton yields are given in Table IV. The neutron yield with π^+ incident is assumed equal to the proton yield for π^-, and vice

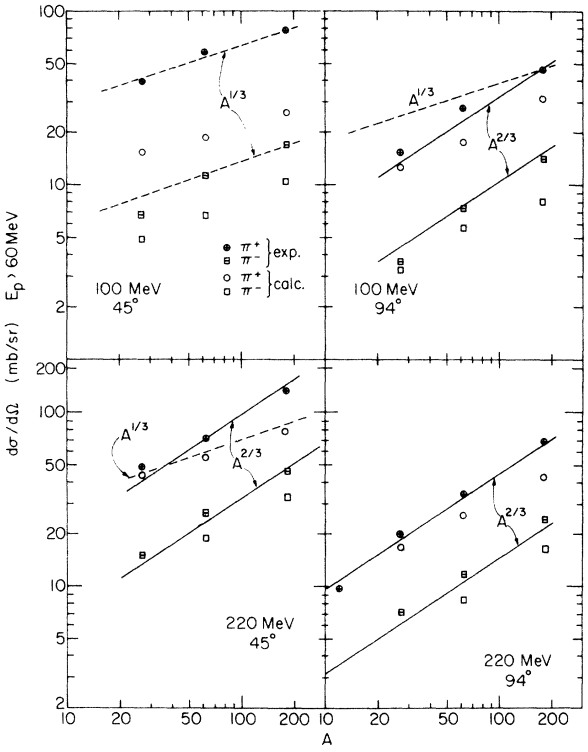

FIG. 10. Integral cross sections for producing protons with energy > 60 MeV as a function of target mass. The open symbols are results of cascade calculations of Ref. 5. The solid lines represent an $A^{2/3}$, the dashed ones an $A^{1/3}$ dependence of the cross section.

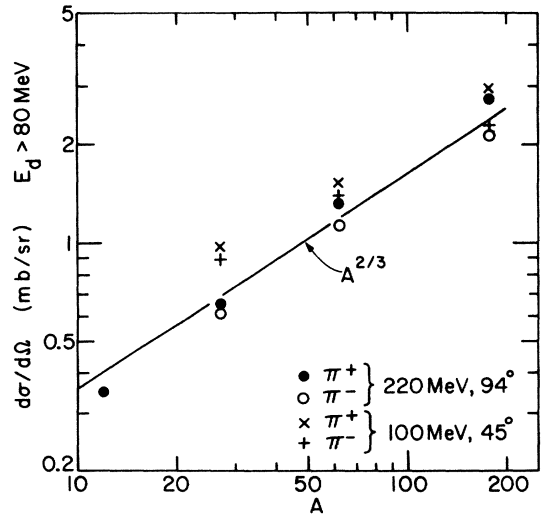

FIG. 11. Same as Fig. 10 for some of the deuteron data, from 100- and 220-MeV pions.

versa. These are based in most cases on the 90° and 45° yields,

$$\sigma_{\text{tot}} \cong \frac{4\pi}{(2+\sqrt{1/2})}\left[2\frac{d\sigma}{d\Omega}(90°)+\sqrt{1}/2\,\frac{d\sigma}{d\Omega}(45°)\right].$$

For 220-MeV π^+ on ^{62}Ni the 120° yield is included, for the others the weights imply a constant $d\sigma/d\Omega$ backwards of 90°. A comparable value estimated from the bubble chamber work of Ref. 8 is also included for 130-MeV π^+ on ^{12}C. Do these rather low cross sections for nucleon production imply that the pion absorption cross section is small (~370 mb for Ni) with two energetic nucleons emerging for each absorption event, or is the absorption cross section large (~750 mb) but with only one energetic nucleon produced per absorbed pion, or are nucleons so heavily degraded by multiple scattering (a very short mean free path after all) that on the average only one emerges from the nucleus with more than 60 MeV? The answer is not clear.

The number of deuterons seen provides an additional piece of information. If these deuterons were produced by pickup reactions induced by the emerging nucleons (as suggested in Ref. 9) one would expect the same spectrum of deuterons with π^+ as with π^- if the target has an equal number of neutrons and protons and if their spatial distributions are the same. But in a heavy nucleus there is a substantial neutron excess, in ^{181}Ta there are almost 50% more neutrons than protons. Thus with an incident π^-, where the primary process produces more high-energy neutrons than protons, one would expect fewer deuterons than with π^+ incident. This difference will be enhanced by the fact that the neutron distribution extends to a larger radius than the charge distribution. There is some evidence for such an effect in Table III.

B. Comparison with cascade calculations

Some guidance on the importance of multiple scattering processes comes from Monte Carlo

TABLE IV. Estimated total cross sections (mb) for producing protons with $E_p \geq 60$ MeV. The uncertainties are those implicit in this averaging procedure, perhaps ~30%.

E_π (MeV)	^{12}C	π^+ ^{27}Al	^{62}Ni	^{181}Ta	π^- ^{27}Al	^{62}Ni	^{181}Ta
100		280	440	680	60	110	190
130	220[a]						
220	180[b]	320	560	1060	110	180	370

[a] From Ref. 8.

[b] From the 90° yield only, assuming the same angular distribution as was seen for ^{27}Al.

calculations using a program that treats the interaction of both the pion and any high-energy nucleons resulting from pion absorption by considering subsequent scatterings in terms of a statistical cascade, using the free π-N and N-N scattering cross sections. This program was described in the literature some time ago[4] and was modified recently.[5] This type of calculation is limited by statistics but it could still provide a useful model of the expected results. Comparisons of proton spectra are made in Fig. 12. Figure 10 shows a comparison of integral yields. The shapes of the proton spectra are more or less reproduced though the statistics in the calculations are much worse than in the data. The total number of events above 60-MeV proton energy in the calculation for a given angle is ~300 for π^+ and ~100 for π^-, so that detailed comparison with the shape of the measured spectra is not very meaningful. As seen in Fig. 10 the absolute cross sections are smaller than the observed ones. The 3 : 1 π^+/π^- ratio is more or less reproduced, the A dependence in the calculations is somewhat less steep than the observed trend. The calculated proton spectra shown in Fig. 12 were corrected for the finite thickness of the detector. The amount of energy deposited in the NaI detector by the higher energy protons was computed and the appropriate number of events were added in the corresponding lower energy bin. These corrected points are shown by open circles.

Two points are worrisome about the cascade calculation. One is that the assumption of free nucleon-nucleon cross sections for the nucleon cascades is likely to result in a much shorter mean free path (1–2 fm) than is generally accepted[15] from the demonstration of nuclear transparency by the nuclear Ramsauer effect.[16] The second is that the calculated pion absorption cross sections are generally very low (e.g., the calculated[5] σ_{abs} of ~190 mb for ^{27}Al at both 100 and 220 MeV may be compared, for instance, with σ_{abs} = 220 mb measured by Belotti *et al.*[8] for the much smaller ^{12}C with 130-MeV π^+).

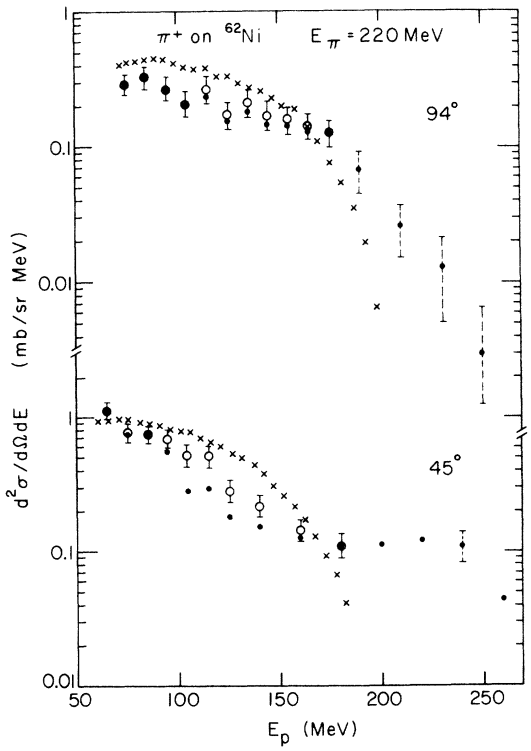

FIG. 12. Comparison of the ^{62}Ni spectra at 220 MeV with the calculated spectra from cascade calculations. The measured cross sections (crosses) should be compared with the open circles, which contain a correction for the finite detector thickness. The uncorrected calculated spectrum is shown by solid dots. The error bars in the calculations are about twice as large as in the data; the experimental errors are not shown.

C. Anomaly at 100 MeV

The discrepancies between the 220-MeV measurements and the cascade calculation are not so glaring that one would feel the need for qualitative remedies to the model. The observed similarity in proton spectra with different targets and pion charge is difficult to check because of the inherently poor statistics in the calculation. Overall, the calculated yields are ~40% low for Ta and about correct for ^{27}Al.

But at 100 MeV the discrepancy becomes more glaring. The calculation predicts an almost isotropic proton yield, while the observed yield is sharply forward peaked for π^+ and somewhat less so for π^-. At 45° the observed yield is three times higher than calculated with π^+. This suggests a qualitative difference in mechanism. Could the longer pion wavelength at this lower energy enhance the sensitivity to correlations between nucleons and give rise to a different mechanism for absorption? More data are needed to explore this behavior.

IV. SUMMARY

The following observations can be made regarding our results.

1. The proton spectra with π^+ and π^- at a given energy and angle are usually similar in shape.

2. The proton yields for $E_p > 60$ MeV are in the ratio of ~3 : 1 for π^+ vs π^- bombardment. This is not easy to understand.

3. The increase in proton yield with target is roughly proportional to $A^{2/3}$, suggesting strong

absorption in one of the two channels and transparency in the other.

4. None of these features (1, 2, and 3) seem to be correct at 45° with 100-MeV pions incident: The proton spectra with π^+ and with π^- have different shapes and the integral yields in the ratio 5 : 1, the dependence on target is $\sim A^{1/3}$.

5. The angle-integrated cross section for ^{62}Ni for the emission of a nucleon with $E \gtrsim 60$ MeV is estimated at 750± 200 mb at 220-MeV and 550 ± 200 mb at 100-MeV pion energy.

6. One energetic deuteron ($E_d \geq 80$ MeV) is seen for about every 30 outgoing nucleons ($E \geq 60$ MeV).

Clearly as more and more information is accumulated our picture of the pion's interactions with complex nuclei becomes better defined. Some of the questions raised by the present results that could readily be answered by simple further experiments are as follows:

A. If the measurements are extended to lighter nuclei (^{12}C and ^{4}He), will the proton spectra continue to look the same? Will the π^+/π^- and deuteron/proton ratios remain roughly constant? Such data will help to elucidate the mechanism of nucleon production and the question of how much nuclear matter participates in the primary absorption process.

B. The 100-MeV pion data look significantly different from those at 220 MeV. Is this the result of a different mechanism in the primary absorption process? Could correlations become increasingly important at lower energies? Some measurements of proton spectra at $E_\pi \cong 50$ MeV would be extremely interesting.

C. Data on the precompound spectra of protons have been obtained in the present experiment for $60 \lesssim E_p \leq 200$ MeV. It would be of interest to obtain similar information on nucleon spectra below 60 MeV and down to the evaporation yield, as well as at the higher energies where the relatively unscattered protons from absorption on two nucleons might be expected.

D. The study of prompt γ rays and radioactivities following fast-pion interactions in the Ni region[3,17] indicate that the distribution of strength among evaporation residues is essentially unchanged between π^+ and π^- bombardment of a given target, while it changes appreciably with the neutron excess of the target. This observation suggests that the isospin difference between the π^+-target and π^--target systems is eradicated during the precompound pion absorption processes, which precede evaporation of any substantial number of nucleons. This would occur, for example, if the same set of nucleon clusters (e.g., $T=0$ two-nucleon pairs or α-like clusters) participated in both π^+ and π^- absorption, and all the nucleons produced by the absorption escaped from the nucleus. If this feature is generally correct, then it further constrains our picture of the absorption process.

Note added in proof. Some of the quantitative differences between the observed proton yields and more recent cascade calculations are reduced over those shown in Fig. 10, but the qualitative discrepancy is still present. We are indebted to J. N. Ginocchio for these results.

We are indebted to J. N. Ginocchio for numerous discussions and for supplying us with the results of his calculations before publication. We also owe thanks to a number of our colleagues for helpful discussions, in particular to M. Peshkin, T. S. H. Lee, H. J. Lipkin, and J. E. Monahan.

---

*Work performed under the auspices of the U. S. ERDA, Division of Physical Research.

†Also at the University of Chicago.

‡Present address: Indiana University, Bloomington, Indiana.

§Also at Argonne National Laboratory.

¶Supported in part by the National Science Foundation.

[1]J. Hüfner, Phys. Rep. 21C, (1975); D. S. Koltun, Advances in Nuclear Physics 3, 71 (1969); M. M. Sternheim and R. R. Silbar, Annu. Rev. Nucl. Sci. 24, 249 (1974).

[2]E. Aslanides, in *Meson-Nuclear Physics*—1976 (Carnegie-Mellon Conference), edited by P. D. Barnes, R. A. Eisenstein, and L. S. Kisslinger (AIP, New York, 1976), Vol. 33, p. 204, and the survey articles cited in Ref. 1; M. D. Cooper, *ibid.*, p. 235; C. B. Dover, *ibid.*, p. 249.

[3]H. E. Jackson, D. G. Kovar, L. Meyer-Schützmeister, S. E. Vigdor, T. P. Wangler, R. E. Segel, J. P. Schiffer, R. L. Burman, P. A. M. Gram, D. M. Drake, V. G. Lind, E. N. Hatch, O. H. Otteson, R. E. McAdams, B. C. Cook, and R. B. Clark, Phys. Rev. Lett. 35, 1170 (1975).

[4]G. D. Harp, K. Chen, G. Friedlander, Z. Fraenkel, and J. M. Miller, Phys. Rev. C 8, 581 (1973).

[5]J. N. Ginocchio (private communication); (unpublished).

[6]E. D. Arthur, W. C. Lam, J. Amato, D. Axen, R. L. Burman, P. Fessenden, R. Macek, J. Oostens, W. Shlaer, S. Sobottka, M. Salomon, and W. Swenson, Phys. Rev. C 11, 332 (1975); J. Favier, T. Bressani, G. Charpak, L. Massonnet, W. E. Meyerhof, and C. Zupancic, Nucl. Phys. A169, 540 (1971).

[7]D. M. Lee, R. C. Minehart, S. E. Sobottka, and K. O. H. Ziock, Nucl. Phys. A182, 20 (1972); M. E. Nordberg, K. F. Kinsey, and R. L. Burman, Phys. Rev. 165, 1096 (1968).

[8]E. Belotti, D. Corvall, and C. Mateazzi, Nuovo Cimento 18A, 75 (1973).

[9]J. F. Amann, P. D. Barnes, M. Doss, S. A. Dytman, R. A. Eisenstein, and A. C. Thompson, Phys. Rev.

Lett. 35, 426 (1975).
[10]R. L. Burman, R. L. Fulton, and M. Jakobson, Nucl. Instrum. Methods 131, 29 (1975).
[11]T. P. Wangler and S. E. Vigdor, Nucl. Instrum. Methods 129, 437 (1975).
[12]B. J. Dropesky, G. W. Butler, C. J. Orth, R. A. Williams, G. Friedlander, M. A. Yates, and S. B. Kaufman, Phys. Rev. Lett. 34, 821 (1975).
[13]C. A. Goulding and J. G. Rogers, Report No. TRI-75-3 (unpublished).
[14]P. D. Barnes (private communication).
[15]A. Bohr and B. R. Mottelson, *Nuclear Structure* (Benjmain, New York, 1969), Vol. 1, p. 165.
[16]J. M. Peterson, Phys. Rev. 125, 955 (1961).
[17]S. E. Vigdor, R. L. Burman, P. A. M. Gram, H. E. Jackson, S. B. Kaufman, R. P. Redwine, L. Meyer-Schützmeister, L. L. Rutledge, Jr., J. P. Schiffer, R. E. Segel, S. L. Tabor, J. N. Worthington, and M. A. Yates, Bull. Am. Phys. Soc. 21, 984 (1976); (unpublished).